optica

Few-cycle lightwave-driven currents in a semiconductor at high repetition rate: supplementary material

FABIAN LANGER,[1,2] YEN-PO LIU,[1,2] ZHE REN,[1,2] VIDAR FLODGREN,[1,2] CHEN GUO,[1] JAN VOGELSANG,[1,2] SARA MIKAELSSON,[1] IVAN SYTCEVICH,[1] JAN AHRENS,[3] ANNE L'HUILLIER,[1] CORD L. ARNOLD,[1] AND ANDERS MIKKELSEN[1,2,*]

[1]*Department of Physics, Lund University, Box 118, 22100 Lund, Sweden*

[2]*Nano Lund, Lund University, Box 118, 22100 Lund, Sweden*

[3]*TEM Messtechnik GmbH, Großer Hillen 38, 30559 Hannover, Germany*

**Corresponding author: anders.mikkelsen@sljus.lu.se*

Published 30 March 2020

This document provides supplementary information to "Few-cycle lightwave-driven currents in a semiconductor at high repetition rate," https://doi.org/10.1364/OPTICA.389150. We start out with a short discussion of proposed theory models. Detailed experimental procedures follow, including the use of the d-scan technique and the influence of the metal contacts.

1. Discussion of theoretical descriptions

The first work by Schiffrin and co-workers [1] invoked a model based on Wannier-Stark localization due to the large optical field strengths. The continuous levels of the conduction and valence band split apart in the external field and adiabatic crossings between them allow the transition of valence band states to conduction band states. This transiently switches the insulating dielectric to a conductive state during an intense half cycle. The asymmetry is achieved by using few-cycle waveforms with differing positive and negative field amplitudes. The description of such an extreme state of matter sensitively relies on the parameters entering the complex and costly calculations [2].

The work by Chen and co-workers [3] relies on a similar mechanism but factors in the effect of the Fermi level of the metal contacts as well. The electric field needs to align the localized states inside the metal gap via the Stark effect with the corresponding states in the electrodes so that a hopping of electrons becomes possible. The field-alignment opens the channel for charge transfer into or out of the semiconductor. This mechanism is different for positive and negative half-cycles owing to the different peak amplitudes resulting from the ultrashort nature of the light pulses. Interestingly, such approaches predict a maximal charge transfer for $\varphi_{CEP} = 0$, when the positive field maximum aligns with the envelope function. This is in contrast to the model used in this study. Judging from the asymmetry introduced by the higher orders of the vector potential, the maximal charge transfer is achieved for $\varphi_{CEP} = \pi/2$. While the absolute CEP is difficult to access experimentally, this could be an interesting parameter for future tests of different theory models.

Given the analogy to coherently photoinjecting carriers by balanced resonant one- and two-photon absorption [4-12], the picture of interfering multiphoton transitions seems more reasonable. Furthermore, we calculate the Keldysh parameter for our experimental parameters to ~1.6 > 1, supporting the multiphoton regime. A prediction for driving multiphoton interference also off-resonantly has been made rather early [13]. Driving this process with a single, broadband laser pulse allows to open multiple interference channels at the same time. We employ the model of ref. 14 due to its simplicity. The only material parameter entering the calculation is the linear and nonlinear refractive index of the material. With a detailed knowledge of the laser pulse shape, we can reproduce the observed behavior to a high level of congruency. This corroborates the validity of this model to describe lightwave-driven-current experiments.

A related modelling approach was proposed by Kruchinin and co-workers [15] and adapted in ref. 16. Here, the underlying process is identified as interfering multiphoton transitions as well. The calculations include the band structure of the material and self-consistently account for dynamic screening of the electric field

inside the material. This approach allows for following the microscopic dynamics in the bands and is capable of explaining even details such as a shift in the charge-maximizing CEP with electric field strength [16].

2. Influence of metal contacts

The metal contacts are formed on gallium nitride via a titanium adhesion layer and a gold layer (see main text). Metal contacts on a semiconductor can result in a space charge region, which could act as a rectifying element. Here, we want to show that we can exclude major influences from static, built-in fields at the contacts in our experiment.

First of all, the laser pulses drive the current in both directions through the metal junction when we continuously change the CEP of the driving pulses with the wedge pair. In the resulting charge traces, we do not observe any differences in positive or negative charge transfers (e.g. Fig. 3c and d of the manuscript). The oscillation is symmetric. Secondly, owing to variations in the fabrication process of the metal contacts, we achieved rather different, static current-voltage characteristics (IV curves) for different device batches. In Fig. S1, we show-case two examples of these IV curves and the resulting charge traces from these devices in the experiment. Both traces look qualitatively similar, although the static electronic properties of the contacts are different. We attribute this fact to the large difference between the optically applied field strength and the static fields. Hence, the measured charge motion is dominated by the optical field and the contacts themselves only play a minor role.

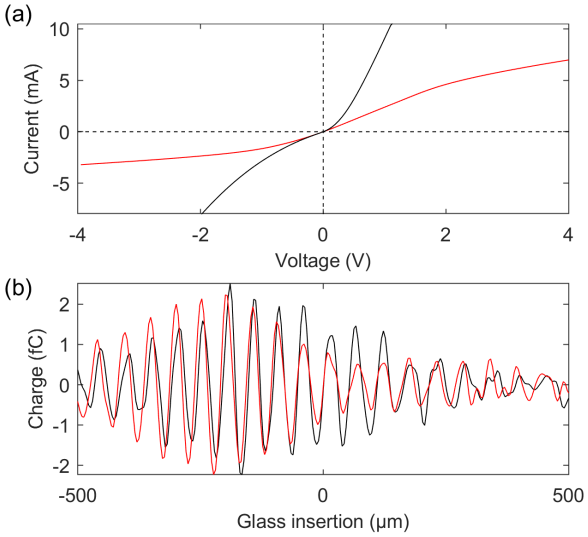

Fig. S1. (a) Static current-voltage characteristic of two different devices (red and black curve) patterned on gallium nitride. While the contacts feature an ohmic behavior for small voltages, they deviate from this behavior substantially for larger voltages and show rather different IVs. (b) The lightwave-induced charge from these two devices is rather similar and their maximally measured charge is almost the same.

3. Experimental procedure

As outlined in the main text, we use an optical parametric chirped pulse amplifier as the source of our driving pulses. The phase of these pulses is actively stabilized in the laser oscillator, operating at a repetition rate of 80 MHz. The stabilization locks the carrier-envelope-offset frequency to 20 MHz. Consequently, every fourth pulse in the train from the oscillator features the same phase, with a constant phase evolution in between. Acousto-optic modulators in the amplifier chain providing the pump pulses for parametric amplification pick selected pulses to down-sample the repetition rate to 200 kHz. By doing so, every 400th pulse from the oscillator is amplified, which results in a phase-stabilized pulse train of identical waveforms.

For our experiments, we want to make use of sensitive lock-in detection and therefore modulate the signal to be measured. This is in accordance with previous works [1,16]. We introduce a phase modulation in the pulse train from the amplifier, so that consecutive pulses feature inverted waveforms. This π-shift in the phase is implemented by picking different pulses for amplification. By choosing every 406th pulse, the repetition rate is set to 197 kHz and the phase inversion in the pulse train is established. In the electronic measurement, the trigger frequency of the lock-in is then set to half the repetition rate and the current signal after the pre-amplifier (see main text) can be measured. We use an integration time constant of the lock-in of 30 ms for most measurements (averaging ~3000 pulses). Acquisition at 10 ms is also easily possible. Since the limiting factor is the translation time of the stage (on the order of 200 ms per step), we have not explored shorter time constants. Using the gain setting of the amplifier (10^5 V/A), we convert the voltage measured by the lock-in into a current flowing in our sample. Dividing the current by the trigger frequency of the lock-in results in the transferred charge per laser shot.

To change the carrier-envelope phase (CEP) of our laser pulses and thereby the current in the sample, we use a glass wedge pair. One wedge is mounted on a linear translation stage. Moving glass in or out of the beam path changes the dispersion of the laser pulses. This not only affects the CEP but also the pulse duration and hence the intensity. The oscillating charge signal can only be observed around the glass insertion for optimally compressed laser pulses.

4. Pulse characterization by the d-scan method

A powerful and convenient method for the characterization of ultrashort laser pulses is the dispersion-scan (d-scan) technique [17,18]. Instead of using an interferometer to split a short pulse into two copies and correlating it with itself in a nonlinear process, the d-scan method uses the dependence of nonlinear processes on

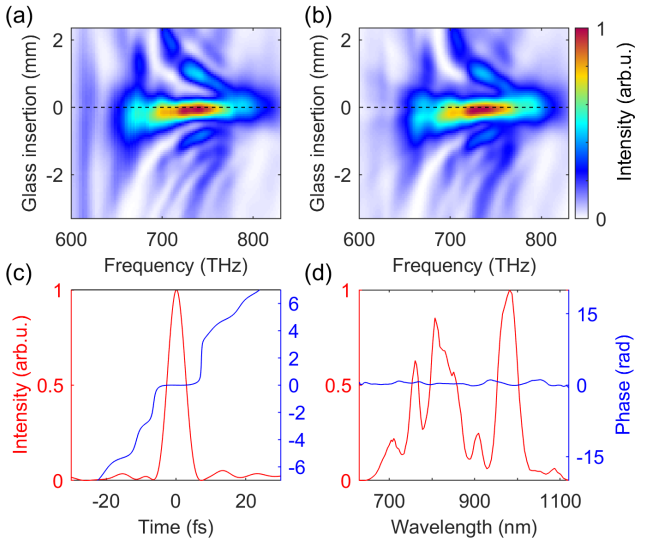

Fig. S2. (a) Measured d-scan for the short pulse. (b) Retrieved d-scan trace. (c) Temporal pulse shape (red) and phase (blue) extracted from the retrieval. The pulse duration is 5.7 fs at the full width at half maximum. (d) Retrieved spectrum (red) and phase (blue).

the pulse shape. In particular, the second-harmonic spectrum changes intensity and shape as a function of the dispersion applied to the fundamental pulses. This nonlinear action can be similarly modelled as in a FROG scan, for example. Here, we record spectra of the second harmonic of our laser pulses as a function of dispersion, by translating the same wedge pair used for measuring lightwave-driven currents. The shorter the pulses, the higher the second-harmonic intensity. But also the shape of the spectrum changes and is different for over-compressed pulses as compared to under-compressed pulses. Making used of established retrieval algorithms, the experiment can be modelled and an optimization routine retrieves the pulse shape by matching the d-scan trace.
This is a crucial part of our experiments. By replacing the gallium nitride sample for lightwave currents with a thin beta-barium borate (BBO) crystal of 5 µm thickness, we directly characterize the laser pulses in the same spot, where the measurements are taken. In that way, we can confidently extract the pulse shape and use a waveform very close to the actually experimentally applied laser pulses for our simulations. It turns out that slight variations in the laser pulse shape and/or spectral phase can lead to a different charge trace in the experiment. We present the d-scans and its retrieval for the short pulse of the manuscript in Fig. S2 (for the d-scan of the long pulse, see Fig. 2 of the manuscript).

5. References

1. A. Schiffrin, T. Paasch-Colberg, N. Karpowicz, V. Apalkov, D. Gerster, S. Mühlbrandt, M. Korbmann, J. Reichert, M. Schultze, S. Holzner, J. V. Barth, R. Kienberger, R. Ernstorfer, V. S. Yakovlev, M. I. Stockman, and F. Krausz, Nature **493,** 70 (2013).
2. A. Schiffrin, T. Paasch-Colberg, N. Karpowicz, V. Apalkov, D. Gerster, S. Mühlbrandt, M. Korbmann, J. Reichert, M. Schultze, S. Holzner, J. V. Barth, R. Kienberger, R. Ernstorfer, V. S. Yakovlev, M. I. Stockman, and F. Krausz, Nature **507,** 386 (2014).
3. L. Chen, Y. Zhang, G. Chen, and I. Franco, Nat. Commun. **9,** 2070 (2018).
4. G. Kurizki, M. Shapiro, and P. Brumer, Phys. Rev. B **39,** 3435 (1989).
5. E. Dupont, P. B. Corkum, H. C. Liu, M. Buchanan, and Z. R. Wasilewski, Phys. Rev. Lett. **74,** 3596 (1995).
6. R. Atanasov, A. Haché, J. L. P. Hughes, H. M. van Driel, and J. E. Sipe, Phys. Rev. Lett. **76,** 1703 (1996).
7. A. Haché, Y. Kostoulas, R. Atanasov, J. L. P. Hughes, J. E. Sipe, and H. M. van Driel, Phys. Rev. Lett. **78,** 306 (1997).
8. T. M. Fortier, P. A. Roos, D. J. Jones, S. T. Cundiff, R. D. R. Bhat, and J. E. Sipe, Phys. Rev. Lett. **92,** 147403 (2004).
9. H. Zhao, E. J. Loren, H. M. van Driel, and A. L. Smirl, Phys. Rev. Lett. **96,** 246601 (2006).
10. J. Rioux, G. Burkard, and J. E. Sipe, Phys. Rev. B **83,** 195406 (2011).
11. E. Sternemann, T. Jostmeier, C. Ruppert, H. T. Duc, T. Meier, and M. Betz, Phys. Rev. B **88,** 165204 (2013).
12. D. A. Bas, K. Vargas-Velez, S. Babakiray, T. A. Johnson, P. Borisov, T. D. Stanescu, D. Lederman, and A. D. Bristow, Appl. Phys. Lett. **106,** 041109 (2015).
13. J. B. Khurgin, Int. J. Nonlinear Opt. Mater. **4,** 163 (1995).
14. J. B. Khurgin, J. Opt. Soc. Am. B **33,** C1 (2016).
15. S. Y. Kruchinin, M. Korbmann, and V. S. Yakovlev, Phys. Rev. B **87,** 115201 (2013).
16. T. Paasch-Colberg, S. Y. Kruchinin, Ö. Sağlam, S. Kapser, S. Cabrini, S. Muehlbrandt, J. Reichert, J. V. Barth, R. Ernstorfer, R. Kienberger, V. S. Yakovlev, N. Karpowicz, and A. Schiffrin, Optica **3,** 1358 (2016).
17. M. Miranda, T. Fordell, C. L. Arnold, A. L'Huillier, and H. Crespo, Optics Express **20,** 688 (2012).
18. M. Miranda, C. L. Arnold, T. Fordell, F. Silva, B. Alonso, R. Weigand, A. L'Huillier, and H. Crespo, Optics Express **20,** 18732 (2012).